Hematoporphyrin monomethyl ether-mediated sonodynamic therapy induces A-253 cell apoptosis

YI ZHANG[1], LIANGJIA BI[1], ZHENG HU[2], WENWU CAO[2,3] and DESHU ZHUANG[1,4]

[1]Department of Stomatology, The Fourth Affiliated Hospital of Harbin Medical University, Harbin, Heilongjiang 150001; [2]Condensed Matter Science and Technology Institute, Harbin Institute of Technology, Harbin, Heilongjiang 150080, P.R. China; [3]Department of Mathematics and Materials Research Institute, The Pennsylvania State University, University Park, PA 16802, USA; [4]Faculty of Dentistry, Department of Oral Biological and Medical Sciences, University of British Columbia, Vancouver, BC V6T 1Z3, Canada

Received August 14, 2019; Accepted January 20, 2020

DOI: 10.3892/ol.2020.11419

Abstract. It has been found that >90% of oral cancer patients suffer from squamous cell carcinoma (SCC). The 5-year survival rate of SCC is ~50%, despite the availability of different treatments. Sonodynamic therapy (SDT) has been developed as a novel therapy for cancer, resisting bacterial infection and inhibiting atherosclerotic plaque progression. The present study investigated the efficacy of hematoporphyrin monomethyl ether (HMME)-mediated SDT on the A-253 epidermoid cancer cell line. The cytotoxicity of HMME and the survival rate of cells following SDT were examined by the MTT assay. Apoptosis and necrosis of cells were detected using flow cytometry with Annexin V and propidium iodide (PI) staining, and fluorescence microscopy with Hoechst 33258 and PI staining. Intracellular reactive oxygen species (ROS) and Ca^{2+} levels were measured using a fluorescence microscope based on 2',7'-dichlorofluorescein diacetate and fluo-3/acetoxymethylester, respectively. Results of the MTT assay demonstrated that a lower concentration (<10 μg/ml) of HMME had no significant effect on the A-253 cells, but SDT combined with ultrasonic treatment for 1 min and 10 μg/ml HMME decreased the cell survival rate by 27%. Flow cytometry analysis revealed that A-253 cells in the SDT group had a higher rate of late apoptosis compared with the control group. Furthermore, fluorescence quantitation of apoptotic A-253 cells demonstrated that the percentages of apoptotic cells were increased in the ultrasound and SDT group compared with those in the control group. In the present study, the ROS level in the SDT group was elevated compared with that in the control group. The Ca^{2+} levels were increased to 181.2 and 268.7% in the ultrasound and SDT groups, respectively, relative to the control group. Taken together, the findings of the present study demonstrated that HMME-SDT significantly induces the apoptosis of A-253 cells together with intracellular ROS generation and Ca^{2+} overload. Thus, HMME-SDT may be a promising treatment option for patients with SCC.

Introduction

Globally in 2018, >90% of oral cancer patients suffer from squamous cell carcinoma (SCC), a malignancy potentially associated with lymph node metastasis (1). SCC starts with variation in mucosal epithelial cells and results in cells with the essential capabilities for malignant growth, loss of cell cycle control and spread (2). Furthermore, the epithelial dysplasia that occurs in SCC reduces the adhesion between cells, which facilitates separation of cells from the tumor and allows metastasis to other organs (3). The 5-year survival rate of SCC is ~50% despite the availability of numerous treatment options, including radiotherapy, chemotherapy and surgical excision (4). A new promising minimally invasive treatment method for patients with SCC is needed due to the damage to the human body, the unreliable efficacy and the side effects of traditional clinical treatments (5).

Sonodynamic therapy (SDT) is an alternative approach for treating patients with SCC that utilizes the synergistic effects of low-intensity ultrasound and sonosensitizers to kill cancer cells, resist bacteria and inhibit atherosclerotic plaque progression (6-8). Hematoporphyrin monomethyl ether (HMME) is an effective sonosensitizer in SDT with a stable structure, lower dark toxicity and higher singlet oxygen yield to induce cell apoptosis via the mitochondrial apoptotic pathway (9). Calcium ion (Ca^{2+}) is a secondary messenger which can regulate apoptosis and a sudden increase of intracellular Ca^{2+} can induce oxidative stress inside the cells (10). During the process of SDT, the sonosensitizer is activated releasing reactive

Correspondence to: Dr Deshu Zhuang, Department of Stomatology, The Fourth Affiliated Hospital of Harbin Medical University, 37 Yiyuan Street, Harbin, Heilongjiang 150001, P.R. China
E-mail: stevenchuang88@126.com

Abbreviations: HMME, hematoporphyrin monomethyl ether; SDT, sonodynamic therapy; ROS, reactive oxygen species; SCC, squamous cell carcinoma; MMP, mitochondrial membrane potential; DCFH-DA, 2',7'-dichlorofluorescein diacetate

Key words: HMME, SDT, ROS, SCC, apoptosis

oxygen species (ROS) that are the principle mediators of cell apoptosis (11,12). However, uncontrolled ROS activity in cells may induce the release of ROS by adjacent mitochondria initiating a positive feedback loop resulting in excessive ROS production leading to mitochondrial injury (13).

Studies have also demonstrated that excessive ROS levels generated during SDT stimulate apoptotic signaling pathways, which include the proteins caspase-3, caspase-9 and Bax (14). During SDT, cell membrane integrity is destroyed together with the loss of the mitochondrial membrane potential (MMP) (15,16). This MMP loss leads to mitochondrial membrane permeabilization (14) and the release of cytochrome *c*, which activates caspase-9, followed by caspase-3 and caspase-7 (17). Some studies have demonstrated that following protoporphyrin IX mediated SDT, human tongue squamous carcinoma SAS cells are arrested at the G_2/M phase of the cell cycle and upregulate p53, which can activate the Fas apoptosis pathway eventually leading to cell death (18,19).

The present study investigated the effect of HMME-mediated SDT on A-253 cells The findings of the present study may facilitate the quest for a promising alternative approach for treating patients with SCC.

Materials and methods

Cell culture. The A-253 cell line is derived from a human submandibular gland epidermoid carcinoma (20). Human SCC A-253 cells were purchased from the American Type Culture Collection and cultured in modified McCoy's 5a medium (American Type Culture Collection) supplemented with 10% fetal bovine serum (Sigma-Aldrich; Merck KGaA.) in an incubator containing 5% CO_2 at 37˚C.

Treatment of cells with HMME. The A-253 cells were incubated in 96-well plates with different concentrations of HMME (0-40 μg/ml at 5 μg/ml intervals) for 90 min in the dark at 37˚C. The sterile HMME solution was supplied by Shanghai Xianhui Pharmaceutical Co., Ltd.

MTT assay. To investigate the cytotoxicity of HMME, cell viability was measured using the MTT assay. Cells at the exponential growth phase were used in each experiment. Overall, 10 μl MTT (5 mg/ml) was added to each well and incubated at 37˚C incubator for 4 h. After removal of the MTT, 1 ml DMSO was added to dissolve the violet formazan crystals. Absorbance at 570 nm was measured using the microplate reader Bio-Tek ELX800 (Biotek Instruments, Inc.).

SDT treatment in vitro. Cell suspension was added to a 3.5-mm petri dish and later positioned in the tank of degassed distilled water ensuring that the cells were 3 cm away from the ultrasound transducer (Fig. 1). The ultrasonic generator, amplifier and transducer utilized in this experiment were supplied by the Harbin Institute of Technology. The ultrasound resonance frequency was 1 MHz, with 30% duty factor and 100 Hz repetition rate, and the ultrasound intensity was 1.5 W/cm^2 as measured by a needle hydrophone (HNC-1000; Onda Corp) inside the well. The temperature change in the medium should not be >1˚C during the experiment. In the present study, MTT

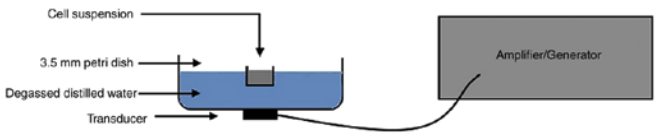

Figure 1. Schematic diagram of the ultrasonic generator and amplifier system used for sonodynamic therapy *in vitro*.

results demonstrated that 10 μg/ml HMME was the optimal concentration to use for *in vitro* SDT treatment. HMME (10 μg/ml) was then applied in combination with different ultrasonic durations (0, 1, 3, 5, 10 and 15 min) to investigate the survival rate of A-253 cells.

Cell apoptosis and necrosis analysis. To investigate cell apoptosis and necrosis following SDT, the Annexin V-FITC apoptosis kit (Merck KGaA) was used for flow cytometry analysis according to the manufacturer's instructions. Subsequently, cells in McCoy's 5a medium were randomly divided into 4 groups: The control group (PBS), the ultrasound group (1 MHz; 1.5 W/cm^2), the HMME group (10 μg/ml) and the SDT group (1 MHz; 1.5 W/cm^2 ultrasound combined with 10 μg/ml HMME). After incubation with HMME or PBS for 90 min at 37˚C, both the ultrasound group and the SDT group were exposed to ultrasound for 1 min at room temperature. After 3 h of treatment, 1x10^6/ml cell per well were then incubated with 5 μl Annexin V and 5 μl PI (Sigma-Aldrich; Merck KGaA) for 10 min at room temperature in the dark. Samples were detected using a FACSCalibur flow cytometer (BD Biosciences). FlowJo version 10 (Tree Star, Inc.) was used to analyze data.

Cell apoptosis and necrosis were also investigated using Hoechst 33258 and PI staining (Merck KGaA) followed by fluorescence microscopy. Firstly, the treated samples were washed with PBS 3 times and then stained according to the manufacturer's protocols. In brief, samples were incubated with 10 μg/ml PI for 10 min at 37˚C in the dark and stained with 5 μg/ml Hoechst 33258 (Merck KGaA)for 5 min. Following incubation, the samples were washed with PBS twice and analyzed using the fluorescence microscope (Zeiss GmbH) at the excitation wavelength of 330-385 nm and the emission wavelength of 420-480 nm at x200 magnification.

Intracellular ROS and Ca^{2+} measurements. The A-253 cells were incubated with 20 μM 2',7'-dichlorofluorescein diacetate (DCFH-DA; Merck KGaA) and 10 μM fluo-3/acetoxymethylester (Merck KGaA) for 30 min at 37˚C to measure the fluorescence of intracellular ROS and Ca^{2+}, respectively. Samples were then washed 3 times with PBS and immediately surveyed using the fluorescence microscope. A total of 1x10^6 cells were collected and measured using a fluorospectrophotometer (Varian Australia Pty, Ltd.) at 488 nm excitation and 525 nm emission wavelengths.

Statistical analysis. All experiments were repeated three times independently and all values were expressed as the mean ± standard deviation. Differences between multiple groups were analyzed using one-way ANOVA, followed by Tukey's post-hoc test. Statistical analyses were performed

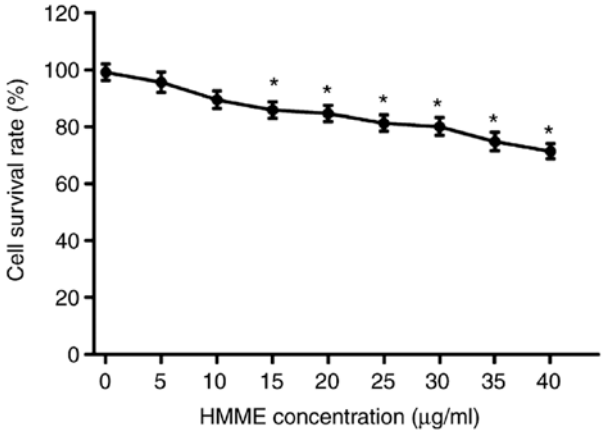

Figure 2. Survival rate of A-253 cells following incubation with different HMME concentrations from 0-40 μg/ml, as determined using the MTT assay. Cells at the exponential growth phase were used in each experiment. Data are presented as the mean ± SD (n=6/group). *P<0.05 compared with the 0 μg/ml HMME group. HMME, hematoporphyrin monomethyl ether.

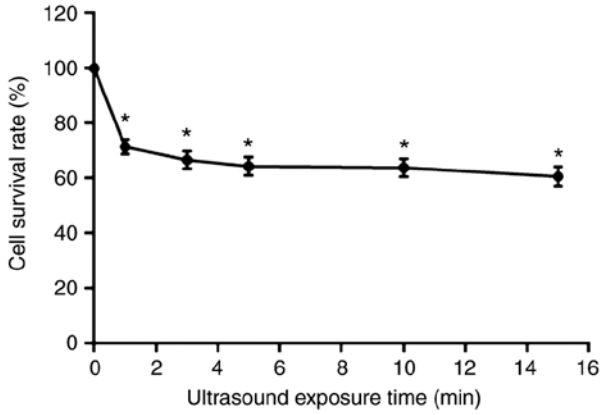

Figure 3. A-253 cell survival rate following incubation with 10 μg/ml hematoporphyrin monomethyl ether plus ultrasound exposure time for 0, 1, 3, 5, 10 and 15 min. Data are presented as the mean ± SD (n=6/group). *P<0.05 compared with the 0 min ultrasound exposure time group.

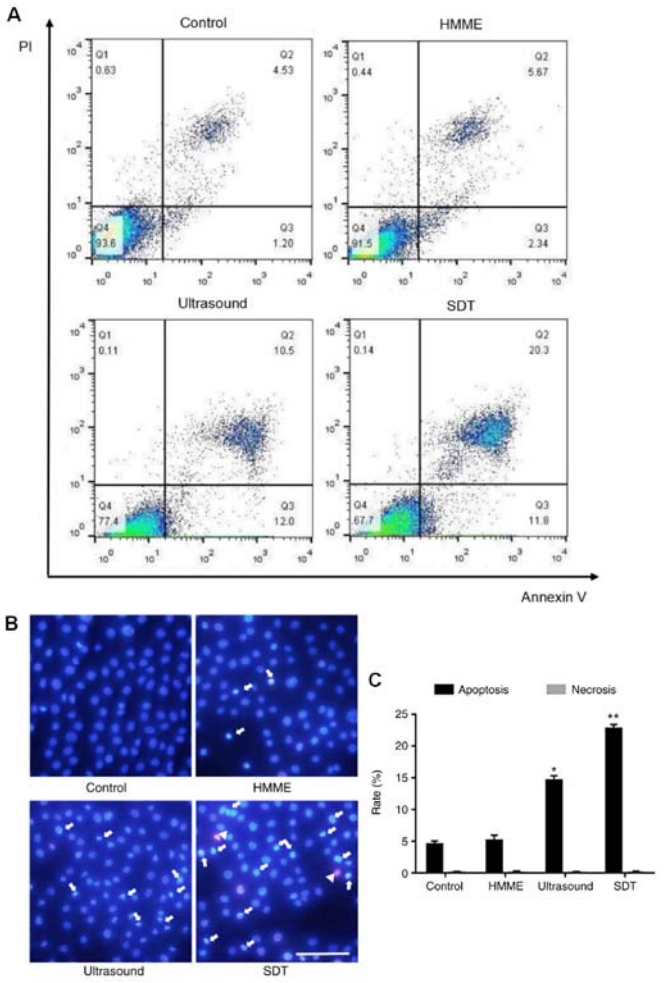

Figure 4. Apoptosis induced by HMME-SDT. (A) Apoptosis rates of A-253 cells measured using flow cytometry with Annexin V and PI double staining. The groups presented are the control, HMME (10 μg/ml), ultrasound (1 min) and SDT (10 μg/ml HMME, 1 min ultrasound exposure) groups. (B) Fluorescence photomicrographs of apoptotic and necrotic A-253 cells with Hoechst 33258 and PI double staining. Normal cells exhibited regular blue fluorescence. Apoptotic cells exhibited bright blue fluorescence (arrows) and necrotic cells exhibited pink fluorescence (arrowheads). Scar bar, 100 μm. (C) Fluorescence quantification of apoptotic and necrotic A-253 cells in control, ultrasound, HMME and SDT groups (n=6/group). *P<0.05 and **P<0.01 compared with the control group. HMME, hematoporphyrin monomethyl ether; SDT, sonodynamic therapy; PI, propidium iodide.

using SPSS version 25.0 (IBM, Corp). P<0.05 was considered to indicate a statistically significant difference.

Results

Increasing HMME concentration decreases A-253 cell survival rates. Cytotoxicity of HMME was measured using the MTT assay. Fig. 2 represents the A-253 cell survival rates at different HMME concentrations. With increasing HMME concentration, the cell survival rate decreased. The lowest cell survival rate was 71% when 40 μg/ml HMME was used. However, HMME concentrations of 5 and 10 μg/ml did not have significant effects on cell survival rates.

Increased ultrasound exposure time during SDT decreases A-253 cell survival rates. Cell survival rates after SDT treatment was also detected by MTT assay. As represented by Fig. 3, the survival rates of A-253 cells following SDT combined with HMME treatment depended on the duration of ultrasound exposure. When the ultrasound exposure time was increased from 1 to 15 min, the survival rate was significantly decreased from 73 to 62% (Fig. 3).

Apoptosis is induced by SDT. Flow cytometry results are represented in Fig. 4A. Cells in the right lower quadrant (Annexin V^+/PI^-) represent early apoptotic cells, those in the right upper quadrant(Annexin V^+/PI^+) represent late apoptotic cells. The apoptosis rates of A-253 cells were as follows: SDT treatment (32.10%), HMME (8.01%) and ultrasound (22.50%) compared with the control group (5.73%) (Fig. 4A). In the double staining with Hoechst 33258 and PI, normal cells displayed regular blue fluorescence, apoptotic cells bright blue fluorescence and necrotic cells pink fluorescence (Fig. 4B). The percentages of apoptotic cells were increased to 14.6% in the ultrasound group (P<0.05) and 22.8% in the SDT group (P<0.01), compared with those in the control group (Fig. 4C).

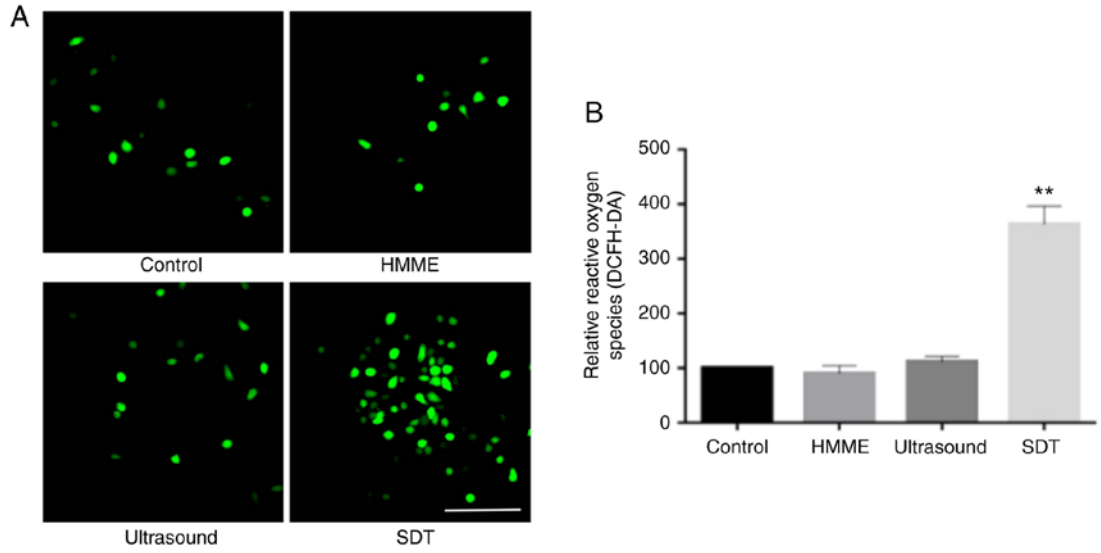

Figure 5. Reactive oxygen species generation induced by SDT. (A) Fluorescence photomicrograph of A-253 cells stained by DCFH-DA. (B) Fluorescence intensity of intracellular ROS was measured by fluorospectrophotometry. Scar bar, 100 μm. Data are presented as the mean ± SD (n=6/group). **P<0.01 compared with the control group. HMME, hematoporphyrin monomethyl ether; SDT, sonodynamic therapy; DCFH-DA, 2',7'-dichlorofluorescein diacetate.

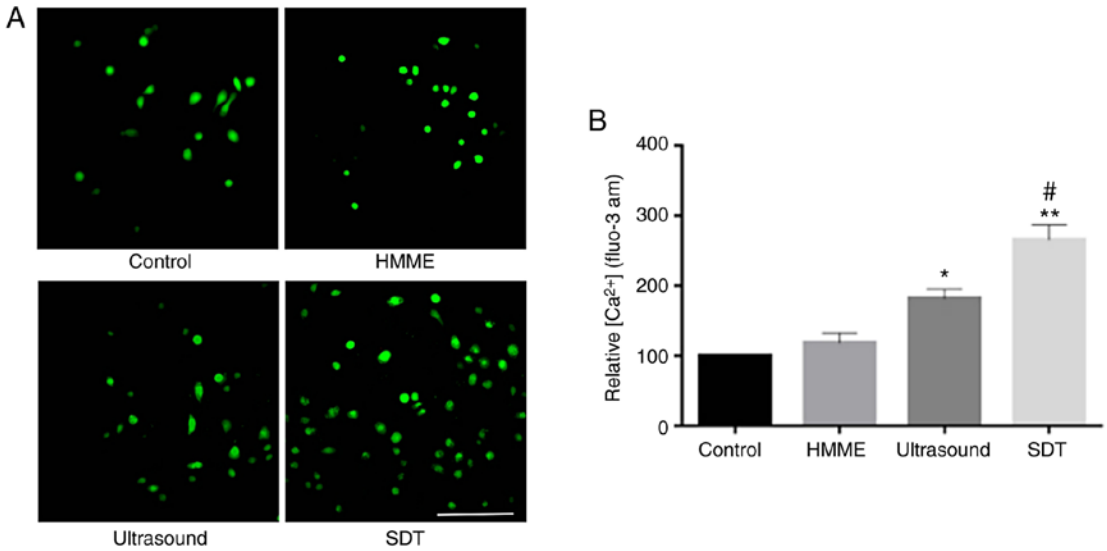

Figure 6. Ca^{2+} generation induced by SDT. (A) Fluorescence photomicrograph of A-253 cells stained by fluo-3/acetoxymethylester. (B) Fluorescence intensity of intracellular Ca^{2+} was measured by fluorospectrophotometry. Scar bar, 100 μm. Data are presented as the mean ± SD (n=6/group). *P<0.05 compared with the control group; **P<0.01 compared with the control group; $^{\#}$P<0.05 compared with the ultrasound group. HMME, hematoporphyrin monomethyl ether; SDT, sonodynamic therapy; Fluo-3 am, fluo-3/acetoxymethylester.

However, the apoptotic rate in the HMME group demonstrated no significant difference compared with the control group. According to the results of fluorescence quantification, very few necrotic cells were identified in all groups (Fig. 4C). Taken together, these results demonstrate that the rate of apoptosis in the A-253 cell line was increased by SDT.

ROS generation increases with SDT. DCFH-DA fluorescence was observed mainly in the SDT group compared with the other 3 groups (Fig. 5A). The ROS level in the SDT group was significantly increased (363.1%; P<0.01), while showing no significant difference in the ultrasound (113.6%; P>0.05) and the HMME (92.5%; P>0.05) groups compared with that in the control group (Fig. 5B).

Calcium overload in A-253 cells treated using SDT and ultrasound. Calcium fluorescence intensity was observed more in the SDT group and to a lower extent in the ultrasound group compared with that in the control group (Fig. 6A). Furthermore, Ca^{2+} levels were increased to 181.2% (P<0.05) and 268.7% (P<0.01) in the ultrasound and SDT groups, respectively, compared with those in the control group (Fig. 6B). Together these results demonstrate that Ca^{2+} levels were significantly increased in A-253 cells following SDT and ultrasound.

Discussion

HMME, a second-generation sonosensitizer, has been extensively utilized in SDT treatment due to its low toxicity and

high selectivity by highly metabolic tissues (21). The optimal concentration of HMME used in the present study is consistent with the results of a previous study that reported the highest cytotoxicity of SDT to U937 cells in the presence of 10 μg/ml HMME (6). Hao *et al* (10) also reported the lowest viability of C6 cells in the presence of 1 MHz ultrasound combined with 10 μg/ml HMME.

It is well documented that apoptosis is the major form of death in numerous types of cancer cells in response to SDT (22,23), which is in accordance with the results of the current study. In the present study, the apoptotic rate in the SDT group was 32.10% ($P<0.05$), while the rates in the HMME and the ultrasound treatment groups were 8.01 and 22.50%, respectively. In addition, the Hoechst 33258 and PI assays confirmed the results of the flow cytometry indicating that the numbers of apoptotic cells were increased in the SDT group compared with those in other groups. During the SDT process, the sonosensitizer is activated and ROS is released; the imbalance between ROS release and elimination may induce further ROS release by the mitochondria (13). This positive feedback results in excess ROS production resulting in mitochondrial injury and apoptosis (24). The ROS level was significantly increased in the SDT group but not in the ultrasound and HMME groups, compared with that in the control group. The findings of the present study indicated that HMME-SDT enhances ROS release and affects cellular conditions of A-253 cells. Notably apoptosis fluorescence was also observed in the ultrasound group confirming previous findings (25). It is well known that ultrasound alone can exert acoustic streaming and cavitation, thereby inducing various biological effects such as exerting shear stresses on the cell membrane, pore formation and endocytosis, leading to induction of cell apoptosis (26).

Ca^{2+} serves a key role as a second messenger in cellular transmission (27). Intracellular Ca^{2+} overload may induce cell apoptosis or death (10). As a result, high intracellular Ca^{2+} levels can be regarded as a signal of early apoptosis (28). The findings of the present study demonstrated that the Ca^{2+} levels were increased in the ultrasound and SDT groups compared with those in the control group. During the process of SDT, cavitation can also occur. When the cell membrane is broken, molecules such as Ca^{2+} can enter the cell by passive diffusion (29). ROS overload may regulate ion channels, including the Ca^{2+} channel, which also induces Ca^{2+} influx (30). These findings may explain the phenomenon of Ca^{2+} overload in both the SDT and ultrasound groups in the current study.

In conclusion, HMME-SDT significantly induces apoptosis, leading to ROS generation and Ca^{2+} overload in A-253 cells. HMME-SDT may be a promising alternative approach in patients with SCC.

Acknowledgements

Not applicable.

Funding

This study was supported by grants from the Natural Science Foundation, Heilongjiang Province of China (no. H2017022) and the Natural Science Foundation of China (no. 81670994).

Availability of data and materials

The datasets used and/or analyzed during the current study are available from the corresponding author on reasonable request.

Authors' contributions

YZ and DZ conceived, designed and performed the experiments. ZH, WC and LB analyzed the data. YZ wrote the manuscript. All authors read and approved the final manuscript.

Ethics approval and consent to participate

Not applicable.

Patient consent for publication

Not applicable.

Competing interests

The authors declare that they have no competing interests.

References

1. Bray F, Ferlay J, Soerjomataram I, Siegel RL, Torre LA and Jemal A: Global cancer statistics 2018: GLOBOCAN estimates of incidence and mortality worldwide for 36 cancers in 185 countries. CA Cancer J Clin 68: 394-424, 2018.
2. Pérez-Sayáns M, Suárez-Peñaranda JM, Gayoso-Diz P, Barros-Angueira F, Gándara-Rey JM and García-García A: The role of p21Waf1/CIP1 as a Cip/Kip type cell-cycle regulator in oral squamous cell carcinoma (Review). Med Oral Patol Oral Cir Bucal 18: e219-e225, 2013.
3. Somasundaram RT, Kaur J, Leong I, MacMillan C, Witterick IJ, Walfish PG and Ralhan R: Subcellular differential expression of Ep-ICD in oral dysplasia and cancer is associated with disease progression and prognosis. BMC Cancer 16: 486, 2016.
4. Taghavi N and Yazdi I: Prognostic factors of survival rate in oral squamous cell carcinoma: Clinical, histologic, genetic and molecular concepts. Arch Iran Med 18: 314-319, 2015.
5. Kerker FA, Adler W, Brunner K, Moest T, Wurm MC, Nkenke E, Neukam FW and von Wilmowsky C: Anatomical locations in the oral cavity where surgical resections of oral squamous cell carcinomas are associated with a close or positive margin-a retrospective study. Clin Oral Investig 22: 1625-1630, 2018.
6. Su X, Wang P, Wang X, Cao B, Li L and Liu Q: Apoptosis of U937 cells induced by hematoporphyrin monomethyl ether-mediated sonodynamic action. Cancer Biother Radiopharm 28: 207-217, 2013.
7. Zhuang D, Hou C, Bi L, Han J, Hao Y, Cao W and Zhou Q: Sonodynamic effects of hematoporphyrin monomethyl ether on staphylococcus aureus in vitro. FEMS Microbiol Lett 361: 174-180, 2014.
8. Yang Y, Liu Y, Chen X, Gong J, Huang Z, Wang W, Shi Y, Wang Y, Yao J, Shen Z, *et al*: 5-aminolevulinic acid-mediated sonodynamic therapy alleviates atherosclerosis via enhancing efferocytosis and facilitating a shift in the Th1/Th2 balance toward Th2 polarization. Cell Physiol Biochem 47: 83-96, 2018.
9. Bilmin K, Kujawska T, Secomski W, Nowicki A and Grieb P: 5-Aminolevulinic acid-mediated sonosensitization of rat RG2 glioma cells in vitro. Folia Neuropathol 54: 234-240, 2016.
10. Hao D, Song Y, Che Z and Liu Q: Calcium overload and in vitro apoptosis of the C6 glioma cells mediated by sonodynamic therapy (hematoporphyrin monomethyl ether and ultrasound). Cell Biochem Biophys 70: 1445-1452, 2014.
11. Su X, Wang P, Yang S, Zhang K, Liu Q and Wang X: Sonodynamic therapy induces the interplay between apoptosis and autophagy in K562 cells through ROS. Int J Biochem Cell Biol 60: 82-92, 2015.

12. Li Y, Zhou Q, Deng Z, Pan M, Liu X, Wu J, Yan F and Zheng H: IR-780 Dye as a sonosensitizer for sonodynamic therapy of breast tumor. Sci Rep 6: 25968, 2016.
13. Bullon P, Cordero MD, Quiles JL, Morillo JM, del Carmen Ramirez-Tortosa M and Battino M: Mitochondrial dysfunction promoted by Porphyromonas gingivalis lipopolysaccharide as a possible link between cardiovascular disease and periodontitis. Free Radic Biol Med 50: 1336-1343, 2011.
14. Wang X, Jia Y, Wang P, Liu Q and Zheng H: Current status and future perspectives of sonodynamic therapy in glioma treatment. Ultrason Sonochem 37: 592-599, 2017.
15. Sun X, Xu H, Shen J, Guo S, Shi S, Dan J, Tian F, Tian Y and Tian Y: Real-time detection of intracellular reactive oxygen species and mitochondrial membrane potential in THP-1 macrophages during ultrasonic irradiation for optimal sonodynamic therapy. Ultrason Sonochem 22: 7-14, 2015.
16. Li Y, Wang P, Zhao P, Zhu S, Wang X and Liu Q: Apoptosis induced by sonodynamic treatment by protoporphyrin IX on MDA-MB-231 cells. Ultrasonics 52: 490-496, 2012.
17. Liu ZR, Chen SQ, Zou YW, Wu XY, Li HY, Wang XQ, Shi Y and Niu HX: Hypochlorite modified albumins promote cell death in the tubule interstitium in rats via mitochondrial damage in obstructive nephropathy and the protective effects of antioxidant peptides. Free Radic Res 52: 616-628, 2018.
18. Li N, Sun M, Wang Y, Lv Y, Hu Z, Cao W, Zheng J and Jiao X: Effect of cell cycle phase on the sensitivity of SAS cells to sonodynamic therapy using low-intensity ultrasound combined with 5-aminolevulinic acid *in vitro*. Mol Med Rep 12: 3177-3183, 2015.
19. Lv Y, Zheng J, Zhou Q, Jia L, Wang C, Liu N, Zhao H, Ji H, Li B and Cao W: Antiproliferative and apoptosis-inducing effect of exo-protoporphyrin IX based sonodynamic therapy on human oral squamous cell carcinoma. Sci Rep 7: 40967, 2017.
20. Sisto M, Lisi S, D'Amore M, Mitolo V and Scagliusi P: Anti-Ro and anti-La autoantibodies induce TNF-alpha production by human salivary gland cells: An in vitro study. Reumatismo 59: 221-226, 2007.
21. Li W, Fei JF, Yang Q, Li BL, Lin C, Yue Q and Meng QG: Acute toxic effects of sonodynamic therapy on hypertrophic scar fibroblasts of rabbit ears. Genet Mol Res 14: 4203-4214, 2015.
22. Xie R, Xu T, Zhu J, Wei X, Zhu W, Li L, Wang Y, Han Y, Zhou J and Bai Y: The combination of glycolytic inhibitor 2-deoxyglucose and microbubbles increases the effect of 5-aminolevulinic acid-sonodynamic therapy in liver cancer cells. Ultrasound Med Biol 43: 2640-2650, 2017.
23. Xiong W, Wang P, Hu J, Jia Y, Wu L, Chen X, Liu Q and Wang X: A new sensitizer DVDMS combined with multiple focused ultrasound treatments: An effective antitumor strategy. Sci Rep 5: 17485, 2015.
24. Sun H, Ge W, Gao X, Wang S, Jiang S, Hu Y, Yu M and Hu S: Apoptosis-promoting effects of hematoporphyrin monomethyl ether-sonodynamic therapy (HMME-SDT) on endometrial cancer. PLoS One 10: e0137980, 2015.
25. Wang F, Gao Q, Guo S, Cheng J, Sun X, Li Q, Wang T, Zhang Z, Cao W and Tian Y: The sonodynamic effect of curcumin on THP-1 cell-derived macrophages. BioMed Res Int 2013: 737264, 2013.
26. Qin P, Han T, Yu ACH and Xu L: Mechanistic understanding the bioeffects of ultrasound-driven microbubbles to enhance macromolecule delivery. J Control Release 272: 169-181, 2018.
27. Li J, Yue W, Huang Z, Chen ZQ, Zhan Q, Ren FB, Liu JY and Fu SB: Calcium overload induces C6 rat glioma cell apoptosis in sonodynamic therapy. Int J Radiat Biol 87: 1061-1066, 2011.
28. Tian J, Gan Y, Pan C, Zhang M, Wang X, Tang X and Peng X: Nerol-induced apoptosis associated with the generation of ROS and Ca^{2+} overload in saprotrophic fungus Aspergillus flavus. Appl Microbiol Biotechnol 102: 6659-6672, 2018.
29. Tran TA, Roger S, Le Guennec JY, Tranquart F and Bouakaz A: Effect of ultrasound-activated microbubbles on the cell electrophysiological properties. Ultrasound Med Biol 33: 158-163, 2007.
30. Lentacker I, De Cock I, Deckers R, De Smedt SC and Moonen CT: Understanding ultrasound induced sonoporation: Definitions and underlying mechanisms. Adv Drug Deliv Rev 72: 49-64, 2014.

This work is licensed under a Creative Commons Attribution-NonCommercial-NoDerivatives 4.0 International (CC BY-NC-ND 4.0) License.